ABSTRACT

Title of Document: Development of Encapsulation Systems from Zein and Metal-

Organic Frameworks (MOFs) for Improved Functional Properties

of Essential Oils

Yunpeng WU (Roc), Master of Science, 2013

Directed By: Assistant Professor, Dr. Qin Wang

Department of Nutrition and Food Science

Essential oils (EOs), which are derived from plants, have antifungal, insecticidal and antimicrobial activities, but they are slightly soluble in water and impart to the water their odor and taste, which limit their applications in food area. Zein, a prolamin from corn, is able to form nanoparticles by liquid-liquid dispersion process. These nanoparticles are well dispersed in water and stable, which can be further applied to encapsulate functional materials that are insoluble in water. We have developed zein nanoparticles to encapsulate thymol and carvacrol in order to improve their solubility. The DLS and SEM proved that zein nanoparticles encapsulated with EO were formed. The particles size was

between 200~300nm before lyophilizing. 65-75% EOs have been encapsulated in the nano-sized particles. DPPH assay results proved good antioxidant property of the product. For the Ferric-ion spectrophotometric assay, hydroxyl free radicals had been cleared by 60~90% in overall. In the antimicrobial experiment, the nanoparticles encapsulating EOs reduced 0.8-1.8 log units of E. coli after 48h incubation.

Furthermore, we have applied Metal-Organic Frameworks (MOFs) to encapsulate thymol. Metal-Organic Frameworks (MOFs) or porous coordination polymers (PCPs) is a new class of hybrid materials, which are formed by the self-assembly of metal-connecting points and polydentate bridging ligands. MOFs in this study was synthetized by Zinc nitrate hexahydrate and 2-aminoterephthalic acid in N, N-dimethylformamide (DMF). Thymol was then loaded inside the MOFs at the loading rate of 3.95%. The structure of porous crystal MOFs was confirmed by scanning electron microscopy (SEM) and X-ray diffraction (XRD). Inhibition to E. coli O157:H7 was measured both in TSB medium and on TSA agar. An E. coli O157:H7 reduction of 4.4 log CFU/mL have been achieved at a thymol to broth ratio of 0.04g/100g. An inhibition area of 223.73 mm^2 was observed after 12h incubation.

With the two methods (zein nano-particles and MOFs), EOs can be encapsulated and well dispersed in water solution. The enhanced antioxidant activity and antimicrobial ability of the encapsulated EOs promise their further applications in food industries.

Development of Encapsulation Systems from Zein and Metal-Organic

Frameworks (MOFs) for Improved Functional Properties of Essential Oils

By

Yunpeng WU (Roc)

Thesis submitted to the Faculty of the Graduate School of the

University of Maryland, College Park, in partial fulfillment

of the requirements for the degree of

Master of Science

2013

Advisory Committee:

Assistant Professor Qin Wang, Chair

Professor Yaguang Luo

Professor Jianghong Meng

Chapter 1: Literature Review

1.1 Introduction of Essential Oils

It has been known that a large number of edible plants have abilities to inhibit the growth of bacteria, yeast and molds or kill them because they contain essential oils (EOs) (Zhu, Zeng et al. 2006; Bernardes, Lucarini et al. 2010). Many researches focus on these compounds and most of them are not available commercially yet. EOs have been widely used as food flavoring agents since ancient times, because most EOs possess strong and unique flavors (Young 2004; Shah, Davidson et al. 2012; Shah, Ikeda et al. 2012). They are generally found in plant's fraction like leaves of thyme, sage, basil, rosemary, and marjoram, flowers or buds of clove, bulbs of garlic and onion, seeds of caraway, fennel, nutgem, and parsley, rhizomes of asafetida, fruits of pepper and cardamom, or other parts of plants (LisBalchin and Deans 1997; Ultee, Bennik et al. 2002; Oliveira, Leitao et al. 2007; Hanif, Bhatti et al. 2010; Kuo, Cheng et al. 2011). As hydrophobic and volatile compounds derived from plants, EOs are considered as natural antifungal, insecticidal, antimicrobial, and antioxidant substances. Due to these admirable properties, EOs have gained much attention and have been studied for a long time. In general, the chemical structure and concentration of EOs affect the antimicrobial efficacy (Chorianopoulos, Giaouris et al. 2008; Gutierrez, Rodriguez et al. 2008). They may kill bacteria cells or inhibit the production of secondary metabolites, like mycotoxins. Phenolic compounds are the antimicrobial components most commonly found in EOs, including terpenes, aliphatic alcohols, aldehydes, ketones, acids, and isoflavonoids. Some EOs are inhibitory against both Gram-positive and Gram-negative bacteria, such as oregano, clove,

cinnamon, and citral. However, most of other EOs are more effective to inhibit Gram-positive than Gram-negative bacteria (Hulin, Mathot et al. 1998; Ho and Su 2012). The chemical analysis of a series of EOs showed that the principal constituents of EOs were citral, eugenol, carvacrol, thymol and their precursors. Ward et al has reported allyl isothiocyanate (AIT) was more effective against Gram-negative bacteria and fungi (Ward, Delaquis et al. 1998) than Gram-positive bacteria. According to the results of Yin et al, garlic oil was also effective against Gram-negative bacteria (Yin and Cheng 2003). Both AIT and garlic oil are nonphenolic constituents of EOs, but still demonstrated promising antimicrobial abilities.

Most of the EOs, as part of the plants' pre- or post-infection defense mechanisms, are partially responsible for combat infectious or parasitic agents. Therefore, if plants demonstrate strong antimicrobial ability, it is probably because they contain EOs that inhibit the growth of microorganisms (Ibrahim, Salameh et al. 2006; Miguel, Cruz et al. 2010).

1.2 Antimicrobial Application of Essential Oils

Plant EOs from nature are usually mixture of several components. With separation and purification, oils showing strong antimicrobial abilities contain high concentrations of eugenol (allspice, clove bud and leaf, bay, and cinnamon leaf), cinnamamic aldehyde (cinnamon bark and cassia oil), and citral (lemon myrtle, Litsea cubeba, and lime) (de Souza, Stamford et al. 2008; Piccirillo, Demiray et al. 2013). The antimicrobial abilities of oregano, thyme and savory are attributed to the volatile terpenes carvacrol, p-cymene, γ-terpinene, and thymol. Borneol and other phenolic compounds from the terpene fraction contribute to the antimicrobial abilities of sage and rosemary (Santurio, da Costa

et al. 2011; Schütze, Boeing et al. 2011). Cumin, caraway, and coriander are responsible for the antimicrobial abilities of Aeromonas hydrophila, Pseudomonas fluorescens, and Staphylococcus aureus. Marjoram and basil can inhibit the growth of B. cereus, Enterobacter aerogenes, Escherichia coli, and Salmonella. Lemon balm and sage EOs are able to inhibit the growth of L. monocytogenes and S. aureus. Sage has antimicrobial abilities because of the terpene thejone, while a group of terpenes (borneol, camphor, 1,8 cineole, a-pinene, camphone, verbenonone, and bornyl acetate) are responsible for the antimicrobial abilities of rosemary(Suhr and Nielsen 2003; Hernandez-Ochoa, Gonzales-Gonzales et al. 2011; Mathlouthi, Bouzaienne et al. 2012; El Bouzidi, Jamali et al. 2013; Hill, Gomes et al. 2013).

Oregano and thyme EOs have been studied to evaluate their antimicrobial abilities against enterobacteria, lactic acid, B. cereus, and Pseudomonas spp. In the past, Pseudomonas species were thought to be highly resistant to botanic antimicrobials. However, Gutierrez et al reported minimum inhibitory concentration (MIC) of oregano and thyme was 425 ppm and 745 ppm, respectively. Caffeine was reported to be an antimicrobial with 0.5% concentration in liquid media (Gutierrez, Rodriguez et al. 2008). Garlic and green tea have been reported to be broad-spectrum bactericidal. Kim et al reported arrowroot tea was effective to kill against E. coli O157:H7 (Kim and Fung 2004).

1.3 Mechanism of Antimicrobial Action of EOs

Although a lot of studies have been done on the possible modes of antimicrobial activities of EOs, the mechanism is still not clear (Dufour, Simmonds et al. 2003; Lee 2009). Di Pasqua et al has reported one possible mechanism to disrupt the bacterial membrane and then kill the bacteria and the concentration can effectively change the antimicrobial

ability of phenolic compounds to denature the membrane protein (Bagci and Digrak 1996; Asili, Emami et al. 2010). The cell permeability was also altered by phenolic compounds to make macromolecules leak from the interior parts. The phenolic compounds could further interfere with cell membrane and cause malfunction of electron transport, nuclein acid synthesis and nutrient uptake. The formation of phenoxyl radicals is thought to be responsible to the antimicrobial ability of EOs. The lack of EOs from fennel, nutmeg and parsley made these EOs less efficient to kill bacteria because alky substituents cannot react with more stable molecules like anethole or ethers myristicin in those plants to form phenoxyl radicals (Chorianopoulos, Giaouris et al. 2008; Paparella, Taccogna et al. 2008; Sarac and Ugur 2008; Zenasni, Bouidida et al. 2008; Bernardes, Lucarini et al. 2010; van Vuuren, du Toit et al. 2010; Tadtong, Suppawat et al. 2012).

Derivative of isothiocynates from onion and garlic was reported to cleave disulfide bonds oxidatively and form the reactive thiocyanate radical, which resulted in inactivating extracellular enzymes (Holley and Patel 2005; Goni, Lopez et al. 2009). Thymol, carvacrol and trans-cinnamaldehyde were reported to cause the disruptive action on plasma membrane and extracellular ATP could be increased by decreasing the intracellular ATP content in E. coli O157:H7. Disturbance of energy production and structural component synthesis could inactivate yeasts. However, biofilms could be formed from the production of exopolysaccharide layers and delay penetration of EOs (Kalemba and Kunicka 2003; Dusan, Marian et al. 2006; Juneja, Dwivedi et al. 2012).

1.4 Application of zein for encapsulation

As one of most important food and industrial crops in the US, corn or maize is a warm-season crop with requirement of warmer temperature to grow than other grains. US alone

consume one-half of world annual production of corn. Endosperm and germ are the major parts of corn kernel as the storage of starch and oil (Kim, Woo et al. 2002; Luo, Zhang et al. 2011).

There are four main ways to process corn: dry milling, wet milling alkaline processing, and the dry grind process to produced ethanol. The latter two are for human consumption. Starch and oil are the main products from wet milling, while dry grind is used mainly for ethanol production. As the major storage protein of corn, zein exists mainly in endosperm and has been used to prepare biodegradable films (Wang, Lin et al. 2005; Quispe-Condori, Saldana et al. 2011; Regier, Taylor et al. 2012). With interesting characteristics of being gouch, hydrophobic, glossy and greaseproof, films made from zein have shown excellent flexibility and compressibility. The physical and mechanical characteristics of zein films have been improved by cross-linking ever since 1960s (Hinchliffe and Kemp 2002; Podaralla and Perumal 2010; Podaralla and Perumal 2012). Zein has been used widely, such as adhesive, biodegradable plastics, chewing gum, coating for food products, fiber, cosmetic powder, microencapsulated pesticides and inks because of its film forming ability and superior biodegradability and biocompatibility. After cast drying, zein tends to form film under acidic treatment and particles under neutral and basic treatment. Zein has been reported to be prepared as microspheres to deliver insulin. Zein can be soluble in aqueous ethanol solution with the ethanol content of 60-85%. By using the different solubility in aqueous ethanol solution, the liquid-liquid dispersion method has been introduced to form the zein nanoparticles, which has been used to encapsulate EOs (Del Nobile, Conte et al. 2008; Ghasemi, Javadi et al. 2012).

1.5 Metal-Organic Frameworks (MOFs)

Metal-Organic Frameworks (MOFs) or porous coordination polymers (PCPs) have gained greater attention recently as a new class of hybrid materials, which are formed by the self-assembly of metal-connecting points and polydentate bridging ligands (Hong, Hwang et al. 2009; Jia, Yuan et al. 2009; Gaudin, Cunha et al. 2012). Many researchers have studied the applications of MOFs in gas storage, atalysis, gas separation and drug delivery. There are crystalline and amorphous MOFs, and the former ones have been studied more because of their crystalline structure and high loading capacity. With recent research about the edible MOFs synthesized by γ-cyclodextrin and potassium ion, it is possible to apply MOFs in food industry (Li, Zhang et al. 2012; Sha, Sun et al. 2012; Sun, Qin et al. 2013). Using different organic linkers, the particle size, morphology and surface area are possible to be tuned for optimization. In general, divalent (Zn^{2+}, Cu^{2+}) or trivalent (Al^{3+}, Cr^{3+}) metal cations are interconnected with the organic linker molecules to form the polyhedral MOFs, resulting in the nanoscale porous cavities. In the past few decades, researchers have focused on developing many porous materials. Zeolite is among them and has the similar structure of MOFs. However, the preparation of zeolites usually requires high temperature (as 400℃ or higher) to remove the template (Juan-Alcaniz, Gascon et al. 2012; Wang, Sun et al. 2012). This limits the application of zeolites embedding materials with bioactivity and low decomposition temperature. In contrast, the nucleation and growth of MOFs can be achieved under relatively mild conditions.

1.6 Objectives of this thesis

Thymol (5-methyl-2-iso-propylphenol) and carvacrol (5-isopropyl-2-methylphenol) are predominant in oregano and thymol oil, respectively. With the similar structure, both

thymol and carvacrol have promising antimicrobial and antioxidant properties because they can disrupt the bacterial membrane and then kill the bacteria. However, thymol and carvacrol have poor solubility in water, which has limited their applications in food area. Therefore, the first objective is to use zein as an encapsulant to form nanoparticles and encapsulate thymol and carvacrol in it, which was found to be very effective and maintain the EOs' antimicrobial and antioxidant properties.

The second objective is to demonstrate a simple surfactant-free postsynthesis loading process of MOFs with thymol. We have synthesized MOF (defined as Zn@MOF) from zinc nitrate hexahydrate and 2-aminoterephthalic acid. Thymol has been loaded into the Zn@MOF pores in N, N-dimethylformamide (DMF) solution. This method produced crystalline Zn@MOF with nanoscale porous cavities loaded with thymol, which were characterized by scanning electron microscopy and porosimeter. The encapsulated thymol has showed promising antimicrobial ability at low concentration.

Both zein nanoparticles loading EOs and the MOFs encapsulating EOs demonstrated promising antimicrobial abilities against food born pathogen at low concentrations.

Chaper 2. Antioxidant and Antimicrobial Properties of Essential Oils Encapsulated in Zein Nanoparticles Prepared by Liquid-Liquid Dispersion Method (Research Paper Published in 2012)

2.1 Materials and methods

Zein sample with a minimum protein content of 97% was obtained from Showa Sangyo (Tokyo, Japan). All chemicals used, including ethanol, ethyl acetate, hydrochloride acid, sodium hydroxide, hydrogen peroxide, phosphate buffered saline (PBS), 2,2-diphenyl-1-picrylhydrazyl radical (DPPH·) and 1,10-phenanthroline-iron (II) were purchased from Sigma - Aldrich (St. Louis, MO, USA). *E. coli* was purchased from ATCC (Manassas, VA), and lysogeny broth (LB) medium was bought from Difco (Franklin Lakes, NJ).

2.1.1 Sample Preparation

Zein and either of the EOs (thymol/carvacral) were dissolved in 70% aqueous ethanol solutions separately to obtain final concentrations of 50 mg/ml and 20 mg/ml, respectively. The stock solutions of zein and EOs were sheared into bulk deionized water using a homogenizer at 17,500 rpm for 2 min. Nitrogen was pumped into solution for 1h to remove the ethanol from the system using a nitrogen evaporator (N-EVAP^{TM}, Organomation Associates, Inc, MA, USA) and then the dispersion was lyophilized (RVT 4104-115, Refrigerated Vapor Trap, Thermo Savant, Waltham, MA, USA) to yield dry powder. Samples treated under different pH conditions were prepared, including acidic pH (4) adjusted with hydrochloride acid, neutral pH (6.5), and basic pH (10) adjusted with sodium hydroxide. Samples encapsulating thymol under different pH conditions (pH

4, 6.5 and 10) were named T4, T6.5 and T10. Similarly, C4, C6.5 and C10 were used for samples encapsulating carvacrol under different pH conditions (pH 4, 6.5 and 10).

2.1.2 Encapsulation Efficiency (EE)

Ethyl acetate was used to extract thymol/carvacrol from dry samples of zein nanoparticles encapsulating thymol/carvacrol, because thymol/carvacrol is soluble in ethyl acetate while zein is not. The standard curve was obtained by dissolving pure thymol/carvacrol in ethyl acetate at a series of mass to volume ratios and reading the absorbance of these solutions at 263nm (for thymol) or 275nm (for carvacrol) using the UV-visible spectrophotometer (Beckman Coulter, DU-730, Fullerton, CA, USA). The standard curve for thymol/carvacrol in ethyl acetate was obtained using ethyl acetate as the blank.

Dry 5 mg samples of zein nanoparticles encapsulating thymol or carvacrol were dissolved in 10 ml ethyl acetate in an ultrasonic bath for 1h and then filtered with a 1µm syringe filter before spectrophotometric assay. The encapsulation efficiency (EE) of essential oils was determined by the following equation (Xiao, Gommel et al. 2011).

EE (% w/w) = Mass of EOs in nanoparticles/Mass of EOs added

2.1.3 Particle Size and Morphology

The particle sizes of samples were obtained by a dynamic light scattering instrument (DLS, BI-200SM, Brookhaven Instruments Corporation, Holtsville, NY, USA). Samples were measured at several stages, including immediately after preparation, after ethanol was removed, and upon re-dispersion after lyophilizing. Samples with different EOs encapsulated under different pH conditions were compared. All measurements were

taken at 20℃ and refractive indices for various aqueous ethanol solutions were applied for autocorrelation to calculate the effective diameter.

Scanning electron microscopy (SEM, SU-70 SEM, Hitachi, Pleasanton, CA, USA) was used to show sample morphology and compare the differences among samples treated at the three pHs and between the two EOs (thymol/carvacrol). After lyophilizing, dry samples were adhered to conductive carbon tapes (Electron Microscopy Sciences, Ft. Washington, PA, USA), and mounted onto specimen stubs coated with a thin (<20 nm) conductive gold and platinum layer using a sputter-coater (Hummer XP, Anatech, CA, USA). Digital images of the samples were obtained and representative images are presented (Figure 2.2).

2.1.4 Fourier Transform Infrared Spectroscopy (FTIR)

FTIR was used to document the changes in chemical structure of zein, EOs and nanoparticle samples. The spectra was acquired at 400 - 4000 cm^{-1} wavenumbers with 1 cm^{-1} resolution utilizing a Jasco 4200 series FTIR spectrophotometer (Jasco Inc., Easton, MD, USA) equipped with a diamond ATR cell.

2.1.5 Solubility test

Solubility of EOs (thymol/carvacrol) was performed as follows (Kim, Jeong et al. 2006; Trapani, Sitterberg et al. 2009): 200 mg EOs was dissolved in 20 ml 70% aqueous ethanol and then dispersed into 40 ml DI water using a homogenizer at 17,500 rpm at different pH values (4, 6.5 and 10). The ethanol was removed using a nitrogen evaporator (N-EVAP^{TM}, Organomation Associates, Inc, MA, USA) for 1h. The insoluble EOs were removed from the aqueous solution by gravity filtration using filter paper (Whatman No.

1) and then the soluble EOs were extracted with ethyl acetate. The ethyl acetate containing EOs was diluted 60 times before measuring absorbance with a UV-visible spectrophotometer (Beckman Coulter, DU-730, Fullerton, CA, USA). The standard curve obtained in part 2.2 was used to determine the maximum concentration of EOs in the water under different pH values. The solubility enhancement was obtained by comparing EO water solubility before and after encapsulation in nanoparticles.

2.1.6 Antioxidant Activity

2,2-diphenyl-1-picrylhydrazyl (DPPH) and 1,10-phenantroline - iron (II) complex free radical-scavenging assays were used for the measurement of antioxidant activity of different samples.

For the DPPH· assay, 0.1 mmol/L DPPH· solution was prepared with 4 mg/ml (effective concentrations of EOs in samples) sample solution prepared in 70% aqueous ethanol. After continuous incubation in the dark at 4℃ for varying lengths of time (0.5h, 1h, 12h and 24h), the DPPH radical scavenging activity of the sample was assessed by measuring absorbance at 517nm against 70% aqueous ethanol as a blank. The control was prepared by replacing the 4mg/ml sample solution with same amount of 70% aqueous ethanol. Also zein without EOs was included as a comparison.

For the 1, 10-phenantroline - iron (II) assay, samples were evaluated for their ability to prevent 1,10-phenanthroline- iron(II) complex ($[Fe(o\text{-}phen)3]^{2+}$) from oxidation by hydrogen peroxide. Since oxidation of Fe (II) was pH sensitive, 10 mM phosphate buffered saline (PBS) was also used. For each test, 1 ml of 1,10-phenanthroline solution in deionized water, 1 ml of $FeSO_4$ solution in deionized water and 1 ml of 0.025% H_2O_2 were mixed with 1ml of 4 mg/ml (effective concentrations of EOs in samples) sample

solution in deionized water and 2 ml of PBS. In the negative control group, 1 ml of PBS was used to replace the sample solution. Also 1 ml PBS was used to replace the 1 ml H_2O_2 in the positive control group. The optical density of each group was measured using the spectrophotometer at 509 nm against a 10 mM PBS blank.

The hydroxyl free radical clearance (percentage) is defined in the Equation below, where A is the Absorbance at 509 nm.

$$\text{Hydroxyl Free Radical Clearance (\%)} = (A_{P\text{-}control} - A_{Sample}) / (A_{P\text{-}control} - A_{N\text{-}control}) \times 100\%$$

Equation 2.1

After the 12 h calculation, the hydroxyl free radical clearance (percentage) was obtained for each sample.

2.1.7 Antimicrobial Ability

Ability of different treatments to inhibit growth of non-pathogenic *E. coli* (ATCC# 53323) was evaluated. The *E. coli* used in this experiment is non-pathogenic, it was selected because of its similarity to well known pathogenic bacteria responsible for many food borne illness outbreaks and clinical infections. *E. coli* were inoculated on lysogeny broth (LB) and samples of the 6 treatments were dispersed in LB medium at an EO to broth w/w ratio of 0.02% . LB inoculated with same amount of *E. coli* without addition of antimicrobial agents was treated as the control. The optical density of each inoculated broth was measured at 550nm using a spectrophotometer. The optical density result can be converted into log CFU/ml, after 12, 24, 36 and 48 hours at 35 ℃ to obtain the inhibition to growth of *E. coli* in comparison to the control, which represents no inhibition.

2.1.8 Statistical analysis

The data reported as mean ± standard error are from experiments conducted in triplicate. Experimental statistics were performed using a SAS software (Version 9.2, SAS Institute Inc., Cary, NC, USA). Analysis of variance (ANOVA) was used to check the assumptions of variance homogeneity and normality and compare the treatment means. Antioxidant activity was analyzed according to a two factor model with 2 levels of EO (thymol/carvacrol) and 3 levels of pH (4, 6.5 and 10) using Tukey's multiple comparison test. The free radical scavenging test was analyzed according to a 3 factor model, with EO, pH and reaction time as the 3 factors using Tukey's Studentized Range (HSD) test to make selected pairwise means comparisons. Differences were considered to be statistically significant for p-values less than or equal to α=0.05.

2.2. Results and Discussion

2.2.1 Encapsulation Efficiency (EE)

EOs were extracted from samples by ethyl acetate which can dissolve EOs (thymol/carvacrol) but not zein (El Babili, Bouajila et al. 2011). The following equations for the standard curves for thymol and carvacrol were obtained. (x stands for the concentration of EOs (mg/ml) and y stands for the absorbance).

Standard curve for thymol: $y = 7.5357x - 0.019$ (R^2=0.9985)

Standard curve for carvacrol: $y = 14.66x - 0.0156$ (R^2 =0.9991)

 Figure 2.1 shows results of the EE: More than 50% of EOs was encapsulated in zein for all treatments using this method. There is no significant difference between the EE for thymol and carvacrol. Although carvacrol has slightly higher solubility than thymol in water, which may result in more release of carvacrol into water, the results show that the

solubility differences do not affect the EE. Since thymol and carvacrol are both volatile essential oils, they were expected to be partially evaporated under low pressure during lyophylizing. Therefore, the real EE should be a little higher than the obtained experimental data. Similar studies about the effect of volatility on encapsulation have shown that more than 90% of non-volatile fish oil could be encapsulated by zein, while only 65-75% of volatile essential oils could be encapsulated (Parris, Cooke et al. 2005; Zhong, Tian et al. 2009).
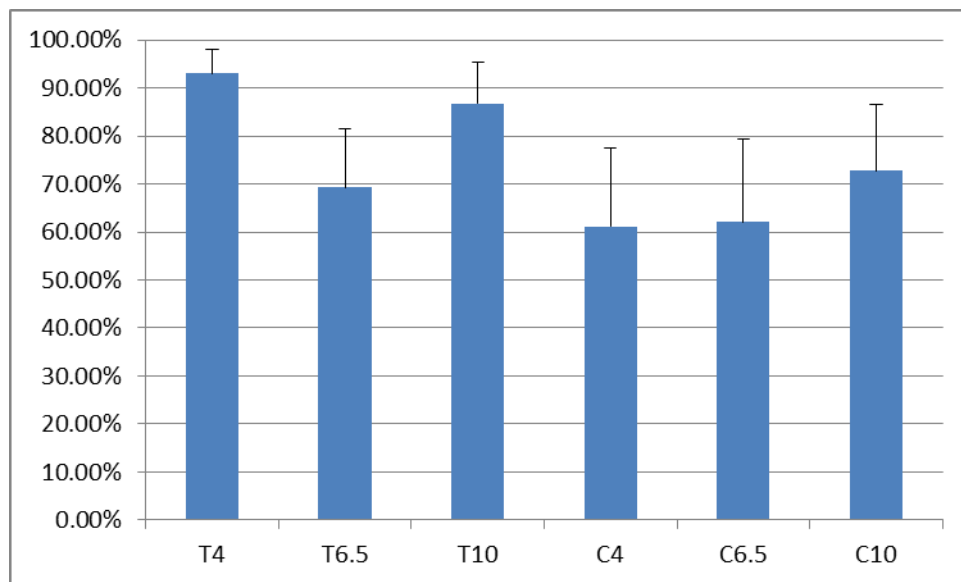
Figure 2.1 Loading efficiency by extracting EOs from samples by ethyl acetate.

2.2.2 Particle Size

DLS was used to determine the particle size before lyophilisation, and after lyophilisation and re-dispersion in water (Table 2.1). The particle sizes of all treatments were kept below 330 nm before lyophilisation and rose a minimum of 160 nm to the range between 430 nm and 740 nm after re-dispersion. The exception was the treatment C10, which had

particle sizes of 52 and 205 nm before and after lyophilisation, respectively. The polydispersity index was relatively low (below 0.3), which ensured the reliability of data from DLS (Dobrynin and Leibler 1997). Particle sizes of all treatments increased after lyophilisation and re-dispersion, indicating that some of the nanoparticles formed by dispersion aggregate during lyophilisation. The samples still remained nano-sized which ensured the good solubility and application in water solution.

Table 2.1

Effective diameter and polydispersity of different samples

	Effective Diameter		Poly Dispersity	
Samples	Before lyophilizing (nm)	Re-dispersion (nm)	Before lyophilizing	Re-dispersion
T4	328.1 ± 21.5	732.2 ± 25.3	0.259 ± 0.023	0.145 ± 0.011
T6.5	269.4 ± 32.9	432.1 ± 43.3	0.136 ± 0.029	0.234 ± 0.021
T10	259.4 ± 59.6	654.2 ± 13.2	0.199 ± 0.032	0.298 ± 0.034
C4	293.6 ± 25.4	490.2 ± 18.2	0.184 ± 0.025	0.321 ± 0.033
C6.5	223.2 ± 42.3	543.8 ± 34.2	0.270 ± 0.008	0.117 ± 0.020
C10	51.9 ± 15.2	205.0 ± 43.3	0.183 ± 0.012	0.229 ± 0.032

2.2.3 SEM Image

SEM images can directly provide information on the particle size and morphology of samples. Figure 2.2 shows the SEM images of zein encapsulating EOs under different pH conditions. It can be seen that the sample morphology was dependent only on the pH no

matter which EOs are encapsulated. The lyophilized samples from acidic solutions formed films (T4 and C4), while nano-scale particles were formed after lyophilizing from neutral and basic solutions with the diameters' ranging from 100nm to 500nm (T6.5, C6.5, T10 and C10). Zhang, Luo et al. (2011) also found that after lyophilizing, zein from acidic solution formed continuous phase of film and zein from near neutral and basic solutions formed dispersed particles.
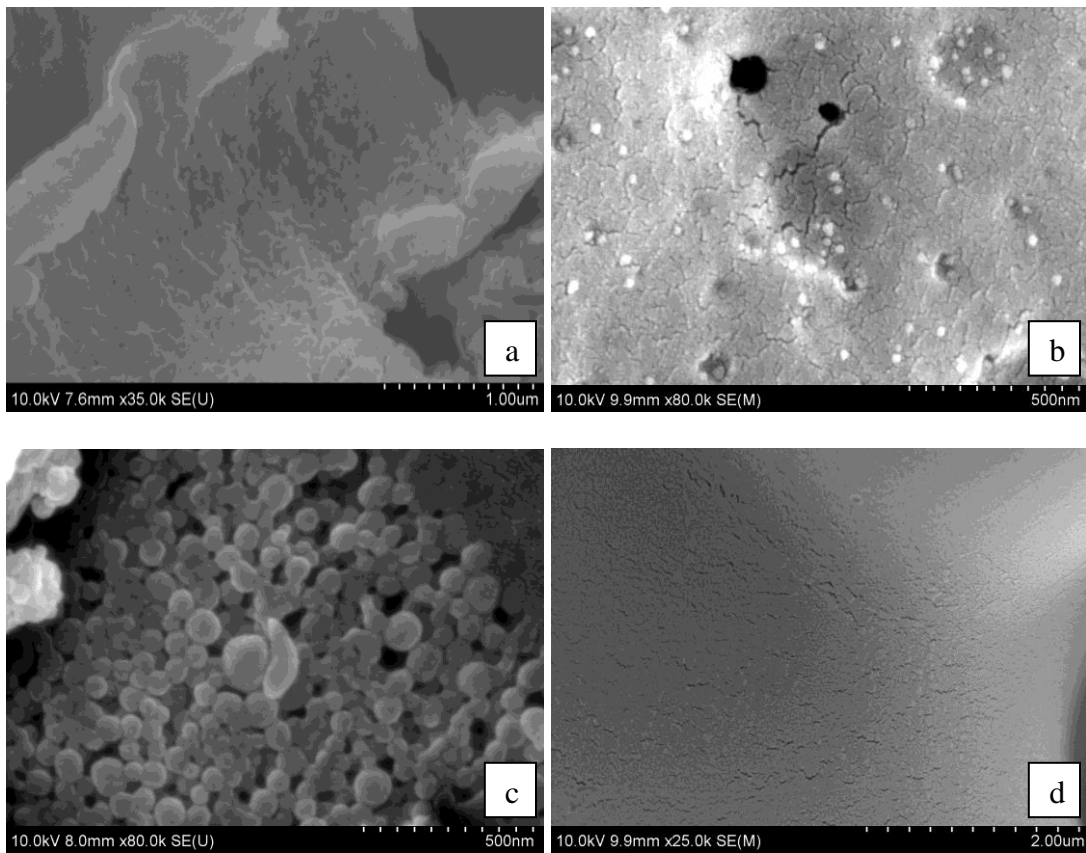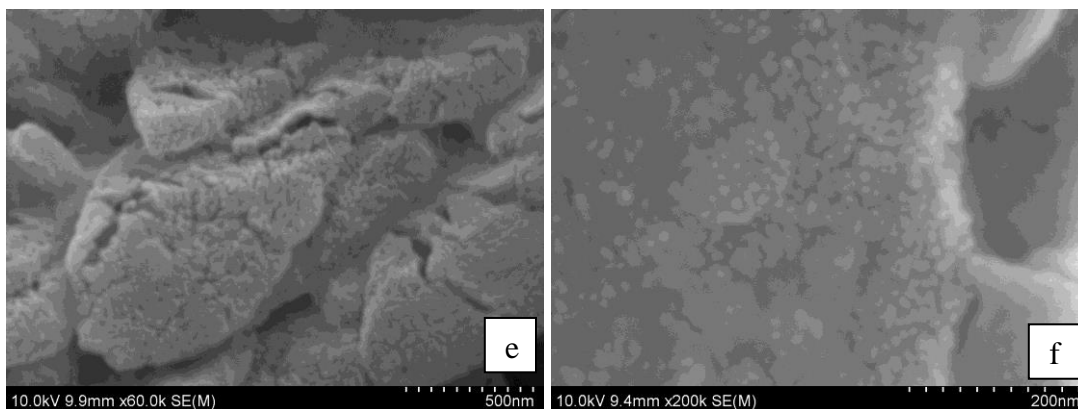
Figure 2.2 SEM image for samples after lyophilizing: (a) T4; (b) T6.5; (c) T10; (d) C4; (e) C6.5; (f) C10

The phase separation (liquid-liquid dispersion) method used in this study was quicker, did not require temperature control, and reagents used to produce nanoparticles were more economical than for other preparation methods, such as chemical conjugation method (Suzuki, Sato et al. 1989) and solid-in-oil-in-water (S/O/W) emulsion process (Morita, Sakamura et al. 2000). Fish oil has been encapsulated by this method with little change in particle size (350 - 450 nm) before lyophilising and after re-dispersing in acetic acid/acetate buffer (Zhong, Tian et al. 2009). EOs (thymol and cinnamaldehyde) have also been encapsulated by phase separation with 0.01% silicone fluid, which resulted in samples between 100 and 250nm after lyophilizing (Parris, Cooke et al. 2005).

Phase separation is an efficient and effective way to form nanoparticles when zein is dissolved in 60~90% (v/v) aqueous ethanol solution to form emulsified droplets. After the stock solution of zein is sheared into bulk water, the concentration of ethanol in the emulsified droplets decreases below the level which can solubilize zein and nano-size particles of zein precipitate (Alargova, Bhatt et al. 2004; Alargova, Paunov et al. 2006).

Encapsulation of EOs in zein nanoparticles allows EOs to be used for many applications that would be otherwise impossible because of their poor solubility in water.

2.2.4 FTIR Spectrum

FTIR provides information of secondary structures of proteins (Bonnier, Rubin et al. 2008) and also is used for EOs analysis (Vera and Chane-Ming 1999). Only the treatments under neutral pH are presented because different pH conditions had no effect on FTIR results.

As shown in Figure 2.3, the peak of zein hydroxyl group ($3287.07cm^{-1}$) merges with that of thymol and carvacrol phenolichydroxyl groups , specifically $3296.71cm^{-1}$ for T6.5 and $3300.57cm^{-1}$ for C6.5. The sharp peaks at $2955.38cm^{-1}$ and $2928.38cm^{-1}$ representing C-H stretching from CH_3 and CH_2 functional groups (Zhang, Luo et al. 2010) merged with peaks at $2962.13cm^{-1}$ and $2957.3cm^{-1}$ for thymol and carvacrol, respectively. In this case, the functional groups responsible for the C-H stretching are the methyl and isopropyl groups on the phenolic rings of EOs (thymol/carvacrol). The four peaks specific to the phenolic ring at wavenumbers ranging from $1622cm^{-1}$ to $1458cm^{-1}$ for thymol/ carvacrol disappeared with the effect of the similar positions of Amide I and Amide II of zein ($1642cm^{-1}$ and $1524.45cm^{-1}$, respectively) (Gillgren, Barker et al. 2009; Kumar, Tripathi et al. 2009).
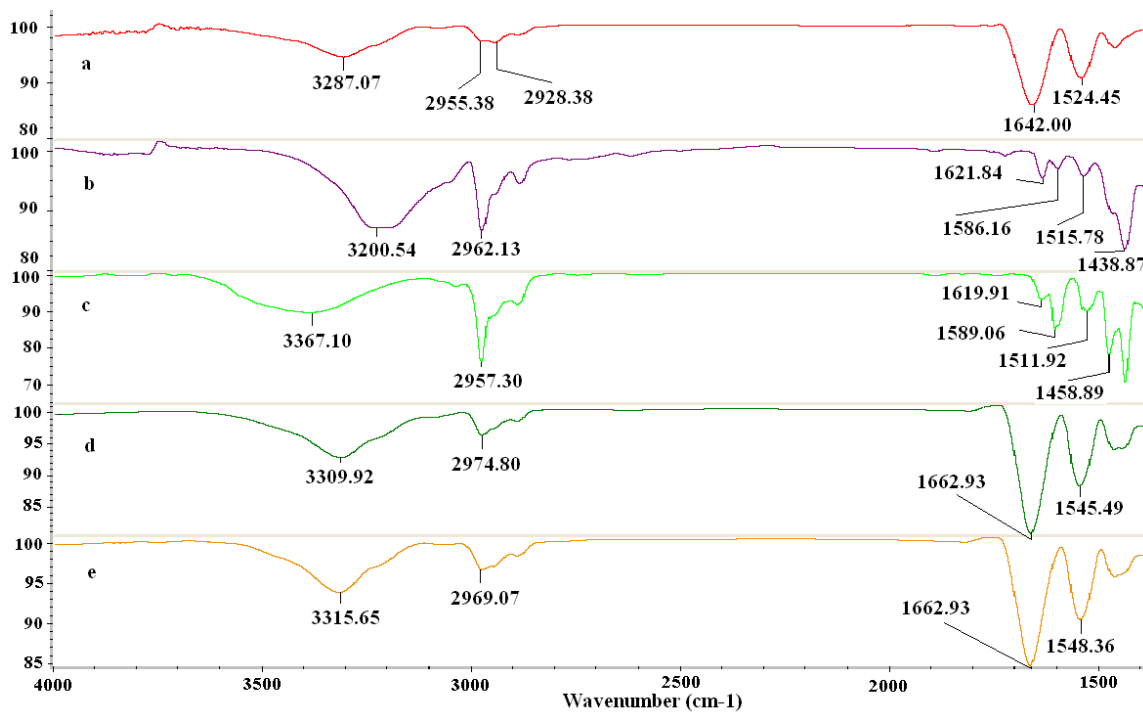
Figure 2.3 FTIR spectrum: (a) zein (b) thymol (c) carvacrol

(d) zein nanoparticles loaded with thymol under pH=6.5 (e) zein nanoparticles loaded

with carvacrol under pH=6.5

All information reflects that no new peaks appeared and that zein and EOs were mixed together physically without any chemical reaction. The structure and function of EOs were not changed in this process, suggesting retention of antioxidant and antimicrobial properties.

2.2.5 Solubility enhancement

The solubility of EOs (thymol/carvacrol) was enhanced by zein encapsulation. All encapsulation treatments regardless of pH conditions showed increased solubility of the EOs ranging from 4-15 folds. Different pH conditions affected the degree of solubility

19

enhancement. The data suggest that solubility of EOs was enhanced least at pH 10. This result can be explained by the deprotonation of the phenolichydroxyl group of EOs under high pH. Some studies also focused on improving the solubility of EOs. Complexation with cyclodextrin has been used to increase the solubility of EOs up to 10 fold (Samperio, Boyer et al. 2010). Water-soluble chitosan (WSC), a polymeric amphiphile favored formation of self-aggregates to carry thymol (Hu, Du et al. 2009). However, EOs in our study were made water soluble neither by forming a complexation, nor by using an amphiphile, but rather by encapsulated in zein nanoparticles.
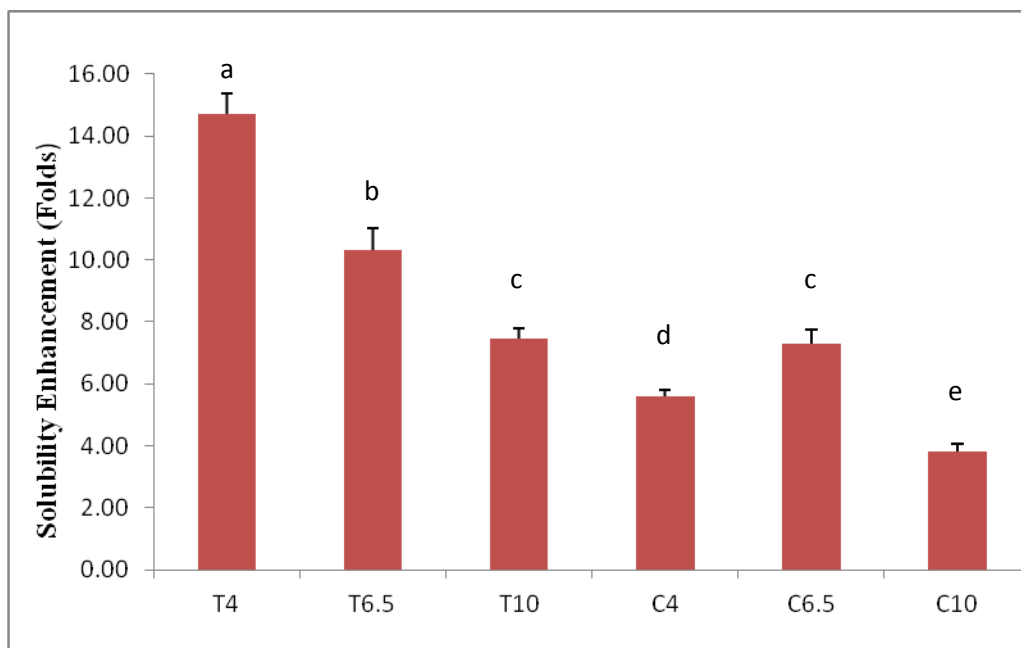

Figure 2.4 Enhancement of solubility of EOs after encapsulation in each treatment. T4, T6.5 and T10 are samples loaded with thymol under pH=4, 6.5 and 10 respectively. C4, C6.5 and C10 are samples loaded with carvacrol under pH=4, 6.5 and 10 respectively.

2.2.6 Antioxidant Capacity

2.2.6.1 DPPH· Assay

All samples showed antioxidant capacity against the 70% aqueous ethanol blank (Figure 2.5). The longer the incubation period, the lower the absorbance of all the samples, as a result of having more time to quench free radicals and bring about a more complete color change. All the samples encapsulating thymol could scavenge free radicals more quickly than those with carvacrol, except C6.5. The mechanism of this assay was based on the reduction of DPPH· by the antioxidant into a colorless substance. After 24h inoculation, 37.5% ~ 75% of DPPH· had been reduced.
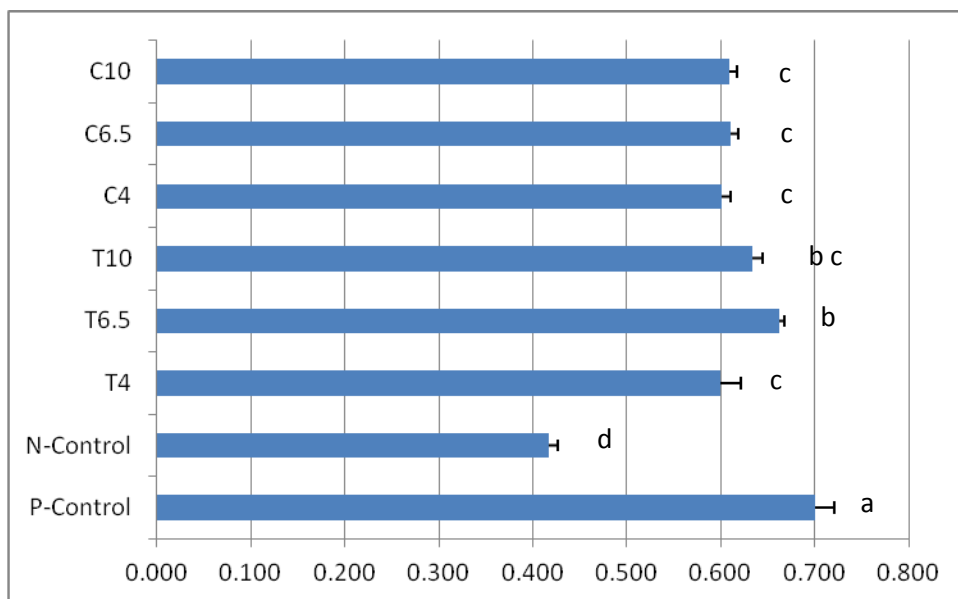

Figure 2.5 DPPH• radical scavenging results of different samples over time by absorbance at 517nm against 70% aqueous ethanol as blank. T4, T6.5 and T10 are samples loaded with thymol under pH=4, 6.5 and 10 respectively. C4, C6.5 and C10 are samples loaded with carvacrol under pH=4, 6.5 and 10 respectively. Means marked with

different letters indicated a significant difference between each other upon the ANOVA

Tukey's Studentized Range Test (P < 0.05)

The antioxidant activity of EOs including thymol and carvacrol has been studied quantitatively by other researchers. Amiri, Yazdi et al. (2011) reported that about 0.1mg/ml of thymol and 0.3mg/ml of carvacrol could provide 50% inhibition of DPPH·. In our study 0.67mg/ml zein encapsulated carvacrol at pH 4 and 10 inhibited 50% of DPPH· and carvacrol at pH 6.5 and thymol at all pH achieved more than 50% inhibition of DPPH·. Zein alone was able to inhibit the free radicals in a related study by Zhang, Luo et al. (2011). The results indicated that zein had slight antioxidant capacity (less than 25% DPPH· reduced after 24h). The zein was also measured in this study at the same concentration. After deducting zein's contribution to the antioxidant capacity, DPPH· was reduced by an additional 24.8% ~ 66.8% among different treatments.

2.2.6.2 Ferric Ion Spectrophotometric Assay

The antioxidant capacity of samples was further demonstrated, by the ferric ion spectrophotometric assay. Results from Figure. 2.6 showed that the $[\text{Fe (o-phen)}_3]^{2+}$ complex was protected by samples from being oxidized by hydrogen peroxide. All samples showed greater antioxidant capacity than the PBS control. PBS was used to prevent ferric or ferrous precipitates, because the ferric ion assay is pH sensitive.

The Hydroxyl Free Radicals Clearance Percentage data were obtained from Equation 2.1, and listed in Table 2.2. There was little difference in HFRC measurement among EOs encapsulated under different pH conditions. In all treatment groups, hydroxyl free radicals were cleared by 60~90%.

Table 2.2

Hydroxyl free radicals clearance (percentage)

EOs	pH	Hydroxyl free radicals clearance %
Thymol	4	64.7 ± 3.9 (a)
	6.5	86.6 ± 8.1 (b)
	10	76.7 ± 8.3 (ab)
Carvacrol	4	65.0 ± 0.3 (b)
	6.5	68.2 ± 6.8 (b)
	10	67.8 ± 6.9 (b)

* Means marked with different letters indicate a significant difference between each other
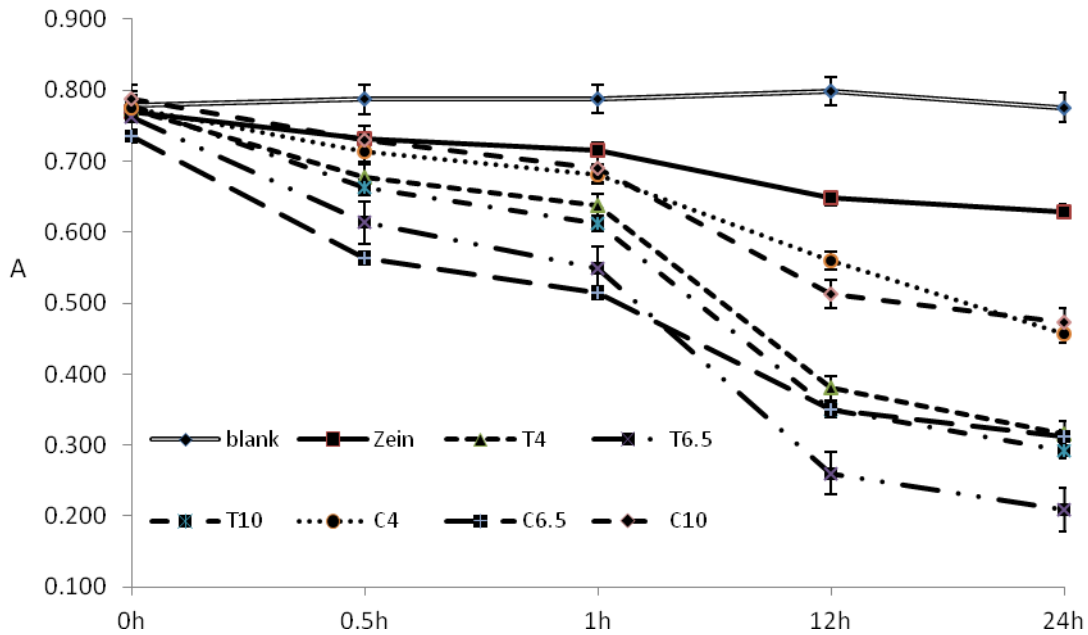
upon the ANOVA Tukey's test ($P < 0.05$).

Figure 2.6 Antioxidant activity of different samples against hydrogen peroxide and the

formation of hydroxyl radicals by absorbance at 509 nm against 10 mM PBS as blank. T4,

T6.5 and T10 are samples loaded with thymol under pH=4, 6.5 and 10 respectively. C4,

C6.5 and C10 are samples loaded with carvacrol under pH=4, 6.5 and 10 respectively.

The antioxidant activity analysis required at least two methods, because of the complexity of the phytochemical reactions (Schlesier, Harwat et al. 2002). Both DPPH· and Ferric ion assays showed that encapsulation did not have much effect on the EOs' antioxidant activity. Thymol antioxidant activity was consistently superior to that of carvacrol, possibly due to greater steric hindrance of the thymol phenolic group (Yanishlieva, Marinova et al. 1999; Viuda-Martos, El Gendy et al. 2010).

2.2.7 Antimicrobial Activity

The in vitro antimicrobial activity of thymol/carvacrol against *E. coli*, a representative Gram-negative bacterium, was evaluated by determining the growth curve in LB medium. Both thymol and carvacrol exhibited interesting antimicrobial activity against *E. coli* after the 48h's incubation in LB medium at 35 °C (Du, Olsen et al. 2008). Thymol and carvacrol both significantly decreased the concentration of *E. coli* by 0.8~1.8 log CFU/ml compared to the control. Although some studies suggest that the release of EOs from zein films can be affected by loaded spelt bran and film's thickness (Mastromatteo, Barbuzzi et al. 2009), zein nanoparticles in this study were found to quickly release all the encapsulated EOs into LB medium. This rapid release is probably the result of the digestion of the zein nanoparticles by *E. coli*.
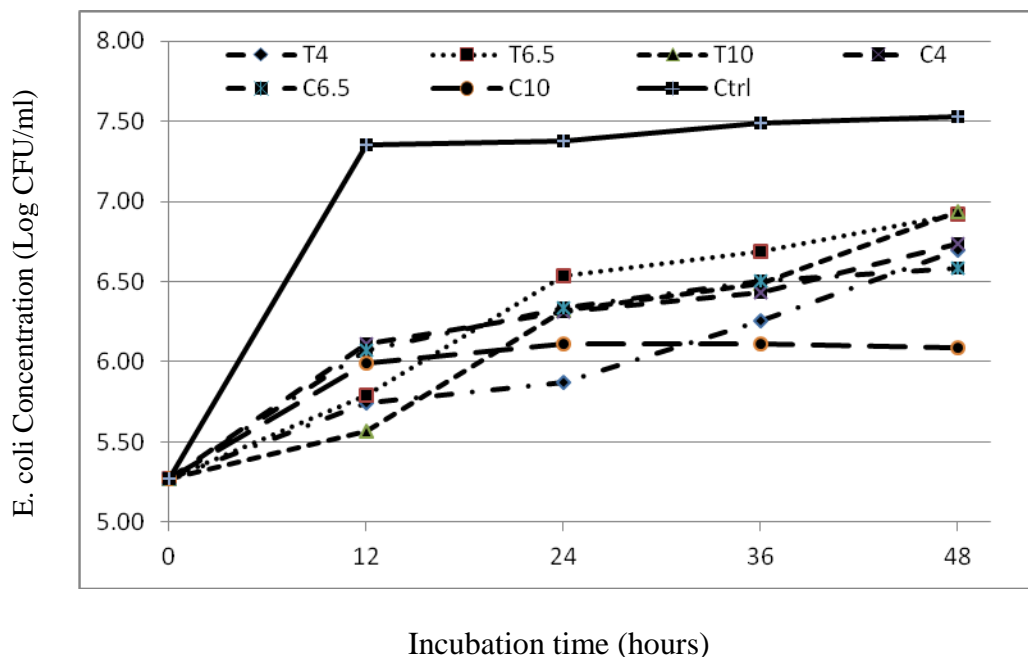
Figure 2.7 Growth curve of E.coli in LB medium with different samples under 35℃. T4, T6.5 and T10 are samples loaded with thymol under pH=4, 6.5 and 10 respectively. C4, C6.5 and C10 are samples loaded with carvacrol under pH=4, 6.5 and 10 respectively.

Thymol and carvacrol have a similar chemical structure, which is responsible for their antimicrobial activity; both contain delocalized electrons and hydroxyl groups on benzene rings. Lambert, Skandamis et al. (2001) proposed that these EOs can break the equilibrium of inorganic ions and pH homeostasis inside the cytoplasm of bacteria. Ultee, Bennik et al. (2002) further demonstrated that carvacrol can act as a transmembrane cation carrier by diffusing through the cytoplasmic membrane, releasing its hydroxyl proton into the cytoplasm, and transporting a potassium ion (or other cation) back across the membrane into the external environment.

Thymol and carvacrol showed different temporal patterns of antimicrobial ability: thymol was consistently more efficient in limiting the growth of *E. coli* than carvacrol under

same pH conditions in the short term (less than 12h), but in the long term, carvacrol achieved better inhibition than thymol except T4 and C4 (as indicated by data at 48h inoculation). Although Ultee, Bennik et al. (2002) reported that the position of hydroxyl group on the phenolic ring has no effect on the antimicrobial ability, our results showed a significant difference (P<0.05). We hypothesize that the position of hydroxyl group may cause differences in polarity and steric hindrance between the thymol and carvacrol molecules, resulting in different ability to interact with *E. coli* cells.

2.3 Conclusions

Essential oils have been studied extensively and there is much literature regarding their desirable antioxidant and antimicrobial properties, however, poor water solubility limits their application. Encapsulation of EOs in zein nanoparticles allows their dispersion in water, which greatly enhances their potential for use in food preservation and control of human pathogenic bacteria. Our study has demonstrated that encapsulating EOs in zein nanoparticles can enhance their solubility up to 14 fold without hindering their ability to scavenge free radicals or to control E. coli growth. Results from this study support the use of nanoencapsulation to facilitate the application of EOs in food preservation.

Chapter 3 Synthesis and Efficacy of Nanoporous Metal-Organic Frameworks (MOFs) Loaded with Thymol as a Bactericide

3.1 MATERIALS & METHODS

Zinc nitrate hexahydrate (98%, reagent grade), 2-aminoterephthalic acid (99%), chloroform (ACS, 99.8%) and N,N-dimethylformamide (DMF, 99%) were purchased from Sigma-Aldrich (St. Louis, MO, USA). *E. coli* was purchased from ATCC (Manassas, VA), while the lysogeny broth (LB) medium was bought from Difco (Franklin Lakes, NJ).

3.1.1 Synthesis of Zn@MOF

Zinc nitrate hexahydrate and 2-aminoterephthalic acid were dissolved in N,N-dimethylformamide (DMF) to obtain final concentrations of 0.018 M (solution A) and 0.006 M (solution B), respectively. After vigorous magnetic stirring of the solutions for 1 h, 10 g A and 10 g B were mixed together in a glass beaker (Yoo, Varela-Guerrero et al. 2011), followed by ultrasonic treatment for 5 min. The precursor solution was then processed solvothermally in a convective oven at 105 ℃ for 24 h. Afterwards, the solution in the glass beaker was cooled to ambient temperature. The solution was then centrifuged at 5000 rpm for 15 minutes to collect the newly formed Zn@MOF crystals. The crystals were then rinsed three times with fresh DMF. In order to remove the DMF inside the Zn@MOF pores, the freshly produced Zn@MOF was soaked in chloroform for 3 days with chloroform replenished every day. After thorough washing with chloroform, the dry Zn@MOF was obtained by evaporating chloroform in the fume hood. The MOFs were stored in a desiccator for further analysis.

3.1.2 Porosity and Surface Area

The porosity and surface area of Zn@MOF were determined by an ASAP 2020 Physisorption Analyzer (Micromeritics Instrument Corporation, Norcross, GA, USA). Sample tubes for analysis were cleaned ultrasonically and dried in a drying oven under 110 ℃. Some Zn@MOF was loaded into a sample tube to degas for 24 h. After degassing, the sample tube containing Zn@MOF was transferred from the degassing port to the analysis port. The analysis was run automatically with N_2 as the adsorptive gas and liquefied N_2 as the cold trap media.

3.1.3 Morphology and X-ray Diffraction (XRD)

Scanning electron microscopy (SEM, SU-70 SEM, Hitachi, Pleasanton, CA, USA) was used to examin the morphology of Zn@MOF. Dry Zn@MOF crystals were adhered to conductive carbon tapes (Electron Microscopy Sciences, Ft. Washington, PA, USA), and mounted onto specimen stubs. The stubs were coated with a thin (<20 nm) conductive gold and platinum layer using a sputter-coater (Hummer XP, Anatech, CA, USA). Digital images of the samples were obtained and representative images were selected for presentation.

X-ray powder Diffraction (XRD) patterns were obtained by XRD diffractometer (C2 Discover Bruker Diffractometer) with CuKα radiation to evaluate the crystalline structure of Zn@MOF.

3.1.4 Preparation of T-Zn@MOF

Fresh Zn@MOF prepared as previously described was sealed in glass bottles with 100 mg thymol /mlchloroform. The mixture was magnetically stirred overnight to insure the

uniform diffusion of thymol. Then the crystals were rinsed with fresh chloroform three times. The chloroform was evaporated in the fume hood to obtain the T-Zn@MOF.

3.1.5 Thermogravimetric Analyses

Thermogravimetric analyses were carried out using a NETZSCH TG 209 F3 instrument (Wittelsbacherstraße 42, 95100 Selb, Germany), with a 10 ℃/min heating rate starting at room temperature and going up to 250 ℃. Dual isotherms were programmed for 10 min at 100 ℃ and 30 min at 250 ℃. A nitrogen atmosphere was used with the 25 mg sample of. All analyses were performed in triplicate.

3.1.6 Antimicrobial Activity

Nonpathogenic *E. coli O157:H7* strains CDC B6914/pGFP (ampicillin resistant), ATCC 43888 were used to evaluate the antimicrobial ability of T-Zn@MOF. A spontaneous nalidixic acid resistant mutant of ATCC 43888 was selected by heavily streaking the parental strains on cefixime, (0.05 mg/L) and potassium tellurite, (2.5 mg/L. Invitrogen, Carlsbad, CA. USA) supplemented sorbital MacConkey (Neugen, Lansing, MIU.S.A) (CT-SMAC) plates. The growth on CT-SMAC plates with / without the antibiotics was quantitatively compared, followed by repeated subculturing without the antibiotics in TSB (Tryptic Soy Broth, Neugen, Lansing, MI, USA) in order to confirm the stability of the antibiotic markers. The nalidixic acid mutant was used instead of the parental strains in the antimicrobial experiment.

3.1.6.1 Growth inhibition against E. Coli O157:H7 in TSB medium

The nalidixic acid mutant of *E. coli O157:H7* was inoculated in TSB with nalidixic acid (50 mg/L). The T-Zn@MOF was dispersed in the inoculation broth at a thymol to broth ratio of 0.04g/100g. Thymol was added to the inoculation broth at a thymol to broth ratio

of 0.04g/100g as the positive control. The TSB inoculation broth containing Zn@MOF without thymol was treated as the negative control. All the treatments were incubated in a shaking incubator at 35℃ for 24 h. The optical density of each inoculated broth was measured at 550 nm using a spectrophotometer. The optical density results were converted into log CFU/mL.

3.1.6.2 Inhibition zone against E. Coli O157:H7 on TSA plate

The Anopore™ inorganic membrane (Anodisc™, diameter 13mm) was used to prepare the inhibition disk. Anodisc™ was placed in DMF before it was thermally treated in a convective oven. A layer of Zn@MOF crystals was grown on the Anodisc™ following the procedure described in *Synthesis of MOFs*. The Anodisc™ with Zn@MOF was washed with chloroform three times before soaking in 100 mg thymol /ml chloroform overnight. The resulting T-Zn@MOF was then washed with chloroform three times and dried in the fume hood to evaporate the chloroform.

The nalidixic acid resistant mutant of *E. coli O157:H7* in Tryptic Soy Broth (TSB) at a concentration of 10^5 CFU/mL (0.1 ml) was plated on Tryptic Soy Agar (TSA) containing 50 mg/L of nalidixic acid . The bacterial inoculum was spread evenly over the plate and left to dry for 10 min in a biosafety hood.

One Anodisc™ saturated with thymol, Zn@MOF or T-Zn@MOF was placed on the center of the inoculated TSA plate. The plates were incubated at 35℃. The inhibition radius around the Anodisc™ was measured using a digital caliper every 12 h. The area of inhibition was then calculated based on the radius.

3.1.7 Statistical analysis

The data reported as mean ± standard error are from experiments conducted in triplicate. Experimental statistics were performed using a SAS software (Version 9.2, SAS Institute Inc., Cary, NC, USA). Analysis of variance (ANOVA) was used to check the assumptions of variance homogeneity and normality and compare the treatment means. Antimicrobial ability was analyzed according to a 4 factor model, with Zn@MOF, Thymol, T-Zn@MOF and control as the 4 factors using Tukey's Studentized Range (HSD) test to make selected pairwise means comparisons. Differences were considered to be statistically significant for p-values less than or equal to $\alpha=0.05$.

3.2 Results and Discussion

3.2.1 Porosity and Surface Area

The N_2 adsorption-desorption isotherms of the Zn@MOF revealed the fine structure of an intraparticle porous topology. The Brunauer–Emmett–Teller (BET) surface area (S_{BET}) of Zn@MOF was determined to be 617.53 m^2/g and the pore opening diameter was 30.01Å. The specific surface areas of different types of MOFs vary depending on different metal ions and organic linkers, for example, Au/ZnO@MOF-5 has S_{BET} of 584 m^2/g (Muller, Turner et al. 2011) and TiO2@MOF-5 has S_{BET} of 2412 m^2/g(Muller, Zhang et al. 2009). The large surface area and pore diameter value provided further evidence of the porous structure of our MOFs (Yoo, Varela-Guerrero et al. 2011). The porous characterization of these MOFs indicated their potential to trap crystalline thymol molecules (Chang, Bristowe et al. 2013).

3.2.2 SEM Images and XRD patterns

SEM images of Zn@MOF presented in Figure 3.2, provide a more direct assessment of particle size and morphology (Zhao, Xia et al. 2011). The crystalline Zn@MOF structure has been formed and may be observed as cubes with sides of about 12 µm (Chen, Wang et al. 2010).
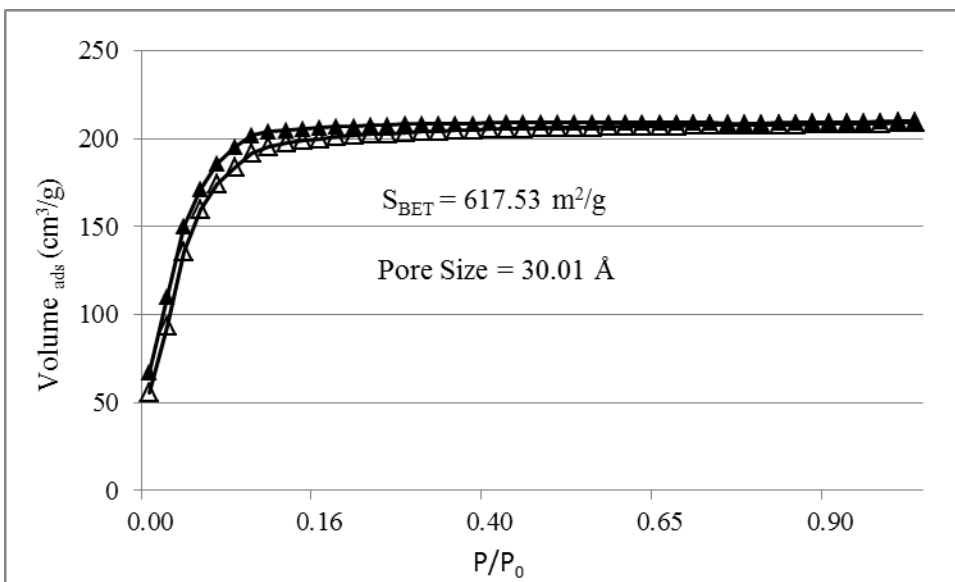
Figure 3.1 N$_2$ sorption isotherms (77 K) for Zn@MOF. Filled and open symbols represent adsorption and desorption traces, respectively. The BET surface area is 617.53 m^2/g and pore size is 30.01Å.
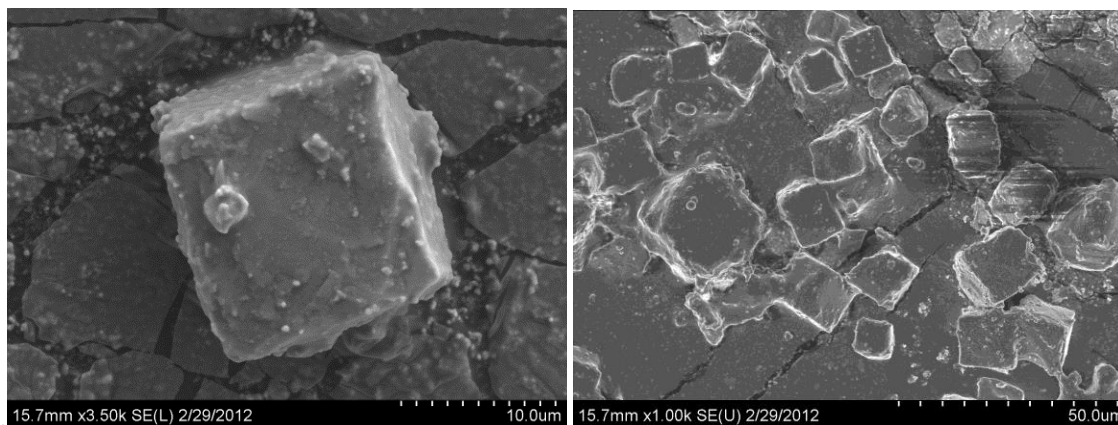

Figure 3.2 SEM images of Zn@MOF.

Figure 3.3 showed that the experimental pattern and the pattern calculated for a cubic body centered lattice with a=18.36 Å matched very well. There was still some residual

difference shown at the bottom in grey. The difference may be due to: 1) distortion of the cubic lattice e.g. in tetragonal or rhombohedral etc fashion; 2) The presence of another minor phase, which for example could be one of the multiple Zn nitrate compounds. Unfortunately, due to the data quality (broad peaks and absence of high angle scattering), it is not feasible to determine the exact cause. Yet it is obvious that Metal-Organic Frameworks were present and could be described as a body-centered lattice with a=18.36 Å (Zhou, Liang et al. 2010; Zhao, Che et al. 2012).
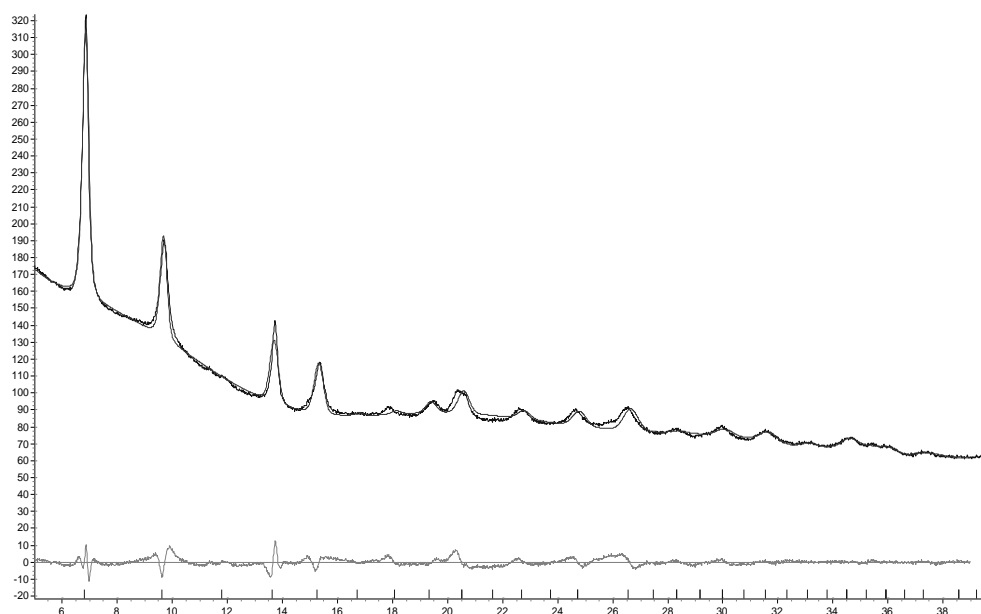

Figure 3.3. XRD patterns of Zn@MOF

SEM and XRD have both been widely used to characterize different MOFs. The porous crystalline structure of MOFs can be decisively confirmed by these two methods (Zhou, Liang et al. 2010; Ploegmakers, Japip et al. 2013).

3.2.3 Thermogravimetric Analyses

TGA is widely used to analyze the materials entrapped inside MOFs, including surfactants (Yoo, Varela-Guerrero et al. 2011) and other solvents like $Zn(OH)_2$ (Chen, Wang et al. 2010). The TGA results (Figure 3.4) indicate that the weight loss took place in the range of 20-100℃ and 100-250℃. The temperature was maintained at 100℃ for 10 min to remove H_2O from T-Zn@MOF. The TGA plot indicates that the 10.66% weight loss between 20 ℃ and 100 ℃ was caused by water desorption. Thymol trapped inside T-Zn@MOF is evaporated at 250 ℃, and corresponds to the 3.95% weight loss. According to the research of Yeonshick et al, the decomposition of organic linker would take place at about 400 ℃ (Yoo, Varela-Guerrero et al. 2011). So Zn@MOF was stable in the process of thermogravimetry. All the thymols have been removed under 250℃ because the boiling point of thymol is 233 ℃. Therefore, the T-Zn@MOF prepared in our study contains 3.95% thymol. Due to itsvolatility, the thymol evaporated at around 150 ℃ (Shah, Ikeda et al. 2012).
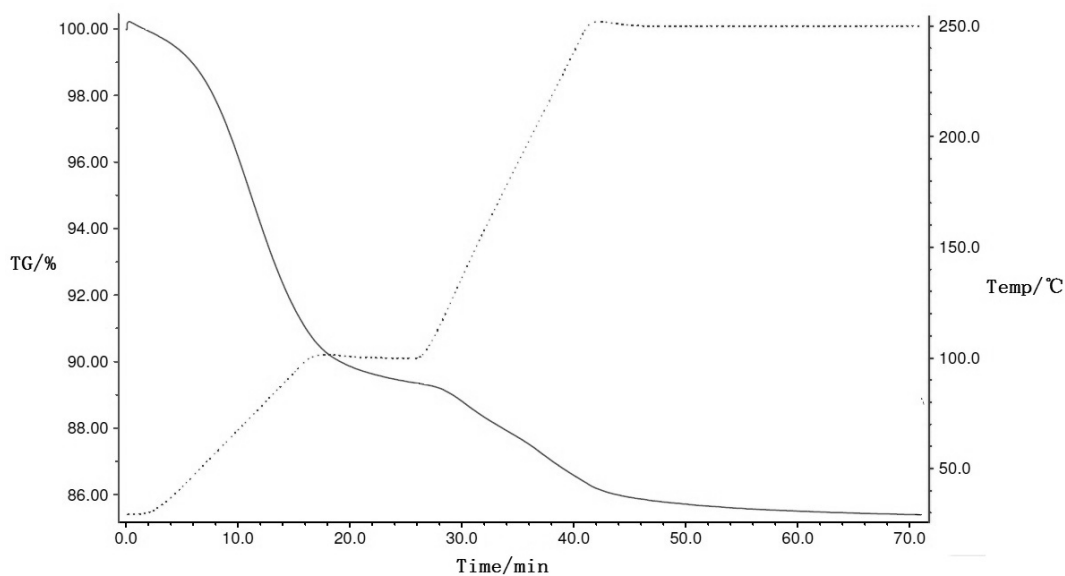
Figure 3.4. Thermogravimetric analyses results, ——TG, ---- Temp.

3.2.4 Antimicrobial Activity

3.2.4.1 Growth inhibition against E. Coli. O157:H7 in TSB medium

The in vitro antimicrobial activity was evaluated by comparing the *E. coli* counts before and after incubation at 35 ℃. From Figure 3.5, T-Zn@MOF (3.95% loading ratio) reduced *E. coli* counts by 4.4 log units (to 0.7 log CFU/mL). Zn@MOF (negative control) showed no significant antimicrobial ability and the antimicrobial ability of thymol alone (positive control; same amount as in T-Zn@MOF) was not as strong as that of the T-Zn@MOF. Thymol in the positive control had only bacteriostatic effect on *E. coli*, but not bactericidal effect (*E. coli* remained 10^5 CFU/mL after 24 h of incubation).
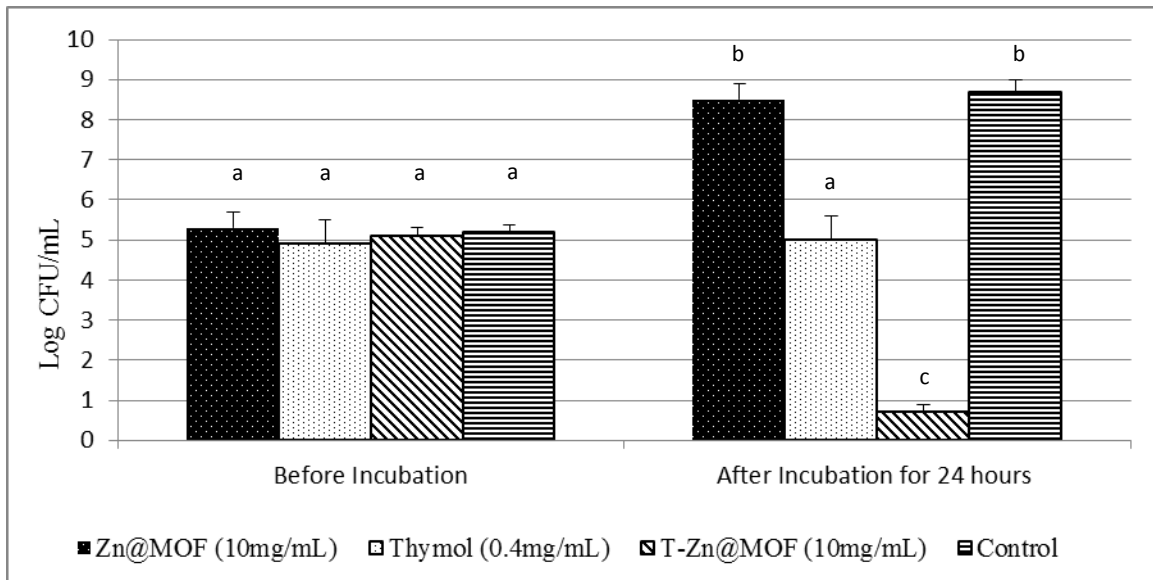

Figure 3.5 Growth inhibition against E. Coli. O157:H7 in TSB medium. Means marked with different letters indicated a significant difference between each other upon the ANOVA Tukey's Studentized Range Test (P < 0.05)

Thymol's delocalized electrons and hydroxyl group on the benzene rings disrupt the equilibrium of inorganic ions and pH homeostasis inside the bacterial cytoplasm. In addition, thymol can release a proton into the cytoplasm and exchange it for a potassium ion which it removes it from the cytoplasm (Ultee, Bennik et al. 2002; Beales 2004), thus causing death of the microorganism. Thymol has gained much attention for its promising antimicrobial ability. However, the poor solubility of thymol has limited its applications, especially in aqueous environments. Our previous study has developed an encapsulation method with zein to enhance the water solubility of thymol and the nanoparticles of zein encapsulating thymol have maintained the antimicrobial activity against *E. coli* (ATCC# 53323). Other researchers have applied techniques like emulsion-evaporation, nanocapsular dispersion and water-soluble chitosan to make thymol soluble in water (Cristani, D'Arrigo et al. 2007; Hu, Du et al. 2009; Shah, Davidson et al. 2012; Shah, Ikeda et al. 2012).

The porous structure of Zn@MOF in this study made it possible to trap thymol inside the crystal Zn@MOF by noncovalent interactions. Release studies have shown that noncovalent loading drugs can be released from MOFs. Thymol's low solubility in water (846±9 ppm) (Griffin, Wyllie et al. 1999; Wu, Luo et al. 2012) reduced the chance for thymol to contact bacteria. This explains why thymol can only inhibit the growth of *E. coli*, but T-Zn@MOF containing the same amount of thymol can kill *E. coli.* The negative control, Zn@MOF did not inhibit *E. coli.*

3.2.4.2 Inhibition zone against E. Coli. O157:H7 on TSA plate

During 72 h incubation at 35℃, *E. coli O157:H7* generally grew normally on TSA with no inhibition zone around the Anodisc™. However, no growth was observed around the

Anodisc™ with T-Zn@MOF. The inhibition zones decreased in area from 223.73 mm^2 to 166.01 mm^2 (Figure 3.6). Abel et al has used bi-axially oriented polypropylene (BOPP) film (20 mm×20mm) coated with thymol to inhibit *E. coli* and detected an inhibition zone with radius of 9.0±0.8 mm (Guarda, Rubilar et al. 2011; Pirbalouti, Rahnama et al. 2011; Ho and Su 2012). Thymol trapped inside Zn@MOF requires media to diffuse into the environment and as a crystallisable phenol moves slower than other non-crystallisable ones, such as carvacrol, which has a similar structure (Sivropoulou, Papanikolaou et al. 1996; Ho and Su 2012). Crystallites hamper the diffusion of molecules and thymol can be released from MOFs continuously, resulting in the slight decrease, by 57.72 mm^2, of the inhibition zone.
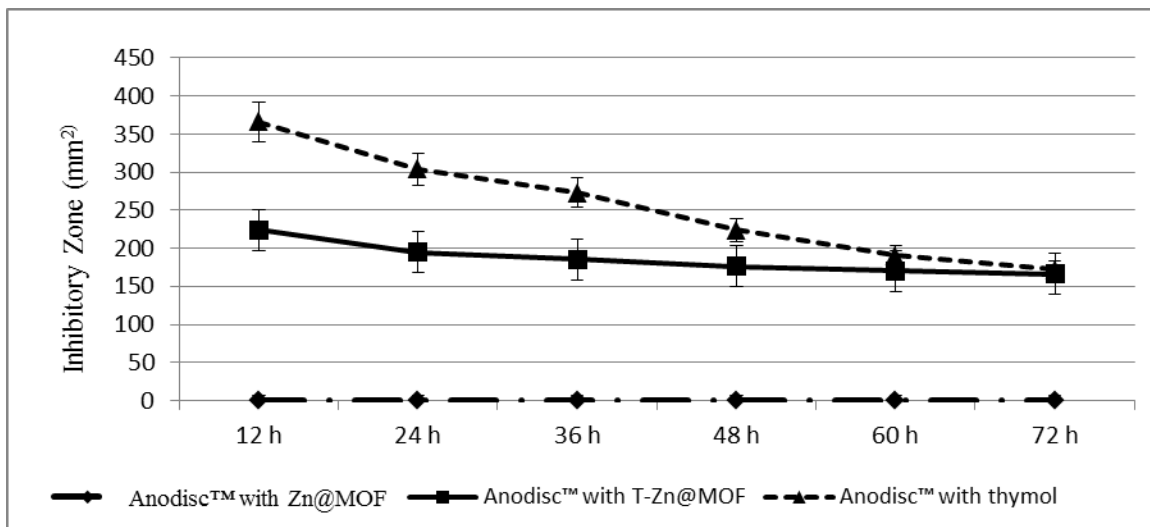

Figure 3.6 Inhibition zone against E. Coli. O157:H7

3.3 Conclusions

Nanoporous Zn@MOF has been successfully synthesized in our study and the morphology has been confirmed by XRD and SEM. Thymol, an effective natural

antimicrobial agent has been loaded into the porous structure of Zn@MOF. During the antimicrobial experiment, T-Zn@MOF was shown to be effective against E. coli O157:H7 at a relatively low thymol concentration. Successful research on edible MOFs and application of MOFs as food additives, suggest that their development has great potential to contribute to food safety in the future.

Bibliography

Alargova, R. G., K. H. Bhatt, et al. (2004). "Scalable synthesis of a new class of polymer microrods by a liquid - Liquid dispersion technique." Advanced Materials **16**(18): 1653-+.

Alargova, R. G., V. N. Paunov, et al. (2006). "Formation of polymer microrods in shear flow by emulsification - Solvent attrition mechanism." Langmuir **22**(2): 765-774.

Asili, J., S. A. Emami, et al. (2010). "Chemical and Antimicrobial Studies of Juniperus sabina L. and Juniperus foetidissima Willd. Essential Oils." Journal of Essential Oil Bearing Plants **13**(1): 25-36.

Bagci, E. and M. Digrak (1996). "Antimicrobial Activity of Essential Oils of some Abies (Fir) Species from Turkey." Flavour and Fragrance Journal **11**(4): 251-256.

Beales, N. (2004). "Adaptation of microorganisms to cold temperatures, weak acid preservatives, low pH, and osmotic stress: A review." Comprehensive Reviews in Food Science and Food Safety **3**(1): 1-20.

Bernardes, W. A., R. Lucarini, et al. (2010). "Antibacterial Activity of the Essential Oil from Rosmarinus officinalis and its Major Components against Oral Pathogens." Zeitschrift Fur Naturforschung Section C-a Journal of Biosciences **65**(9-10): 588-593.

Bonnier, F., S. Rubin, et al. (2008). "FTIR protein secondary structure analysis of human ascending aortic tissues." Journal of Biophotonics **1**(3): 204-214.

Chang, B. K., P. D. Bristowe, et al. (2013). "Computational studies on the adsorption of CO_2 in the flexible perfluorinated metal-organic framework zinc 1,2-bis(4-pyridyl)ethane tetrafluoroterephthalate." Physical Chemistry Chemical Physics **15**(1): 176-182.

Chen, B., X. J. Wang, et al. (2010). "Synthesis and characterization of the interpenetrated MOF-5." Journal of Materials Chemistry **20**(18): 3758-3767.

Chorianopoulos, N. G., E. D. Giaouris, et al. (2008). "Disinfectant test against monoculture and mixed-culture biofilms composed of technological, spoilage and pathogenic bacteria: bactericidal effect of essential oil and hydrosol of Satureja thymbra and comparison with standard acid-base sanitizers." Journal of Applied Microbiology **104**(6): 1586-1596.

Cristani, M., M. D'Arrigo, et al. (2007). "Interaction of four monoterpenes contained in essential oils with model membranes: Implications for their antibacterial activity." Journal of Agricultural and Food Chemistry **55**(15): 6300-6308.

de Souza, E. L., T. L. M. Stamford, et al. (2008). "Interference of heating on the antimicrobial activity and chemical composition of Origanum vulgare L. (Lamiaceae) essential oil." Ciencia E Tecnologia De Alimentos **28**(2): 418-422.

Del Nobile, M. A., A. Conte, et al. (2008). "Antimicrobial efficacy and release kinetics of thymol from zein films." Journal of Food Engineering **89**(1): 57-63.

Dobrynin, A. V. and L. Leibler (1997). "Theory of polydisperse multiblock copolymers." Macromolecules **30**(16): 4756-4765.

Du, W. X., C. W. Olsen, et al. (2008). "Storage stability and antibacterial activity against Escherichia coli O157 : H7 of carvacrol in edible apple films made by two different casting methods." Journal of Agricultural and Food Chemistry **56**(9): 3082-3088.

Dufour, M., R. S. Simmonds, et al. (2003). "Development of a method to quantify in vitro the synergistic activity of "natural" antimicrobials." International Journal of Food Microbiology **85**(3): 249-258.

Dusan, F., S. Marian, et al. (2006). "Essential oils - their antimicrobial activity against Escherichia coli and effect on intestinal cell viability." Toxicology in Vitro **20**(8): 1435-1445.

El Babili, F., J. Bouajila, et al. (2011). "Oregano: Chemical Analysis and Evaluation of Its Antimalarial, Antioxidant, and Cytotoxic Activities." Journal of Food Science **76**(3): C512-C518.

El Bouzidi, L., C. A. Jamali, et al. (2013). "Chemical composition, antioxidant and antimicrobial activities of essential oils obtained from wild and cultivated Moroccan Thymus species." Industrial Crops and Products **43**: 450-456.

Gaudin, C., D. Cunha, et al. (2012). "A quantitative structure activity relationship approach to probe the influence of the functionalization on the drug encapsulation of porous metal-organic frameworks." Microporous and Mesoporous Materials **157**: 124-130.

Ghasemi, S., N. H. S. Javadi, et al. (2012). "Investigation on Development of Zein Antimicrobial Edible Film and Essential Oil of Zataria multiflora Boiss. on Sallmonella enteritidis, Listeria monoeytogenes, Escherichia coli and Staphylococcus aureus." Asian Journal of Chemistry **24**(12): 5941-5942.

Gillgren, T., S. A. Barker, et al. (2009). "Plasticization of Zein: A Thermomechanical, FTIR, and Dielectric Study." Biomacromolecules **10**(5): 1135-1139.

Goni, P., P. Lopez, et al. (2009). "Antimicrobial activity in the vapour phase of a combination of cinnamon and clove essential oils." Food Chemistry **116**(4): 982-989.

Griffin, S. G., S. G. Wyllie, et al. (1999). "The role of structure and molecular properties of terpenoids in determining their antimicrobial activity." Flavour and Fragrance Journal **14**(5): 322-332.

Guarda, A., J. F. Rubilar, et al. (2011). "The antimicrobial activity of microencapsulated thymol and carvacrol." International Journal of Food Microbiology **146**(2): 144-150.

Gutierrez, J., G. Rodriguez, et al. (2008). "Efficacy of plant essential oils against foodborne pathogens and spoilage bacteria associated with ready-to-eat vegetables: Antimicrobial and sensory screening." Journal of Food Protection **71**(9): 1846-1854.

Hanif, M. A., H. N. Bhatti, et al. (2010). "Antibacterial and Antifungal Activities of Essential Oils Extracted from Medicinal Plants Using CO2 Supercritical Fluid Extraction Technology." Asian Journal of Chemistry **22**(10): 7787-7798.

Hernandez-Ochoa, L., A. Gonzales-Gonzales, et al. (2011). "STUDY OF THE ANTIBACTERIAL ACTIVITY OF CHITOSAN-BASED FILMS PREPARED WITH DIFFERENT MOLECULAR WEIGHTS INCLUDING SPICES ESSENTIAL OILS AND FUNCTIONAL EXTRACTS AS ANTIMICROBIAL AGENTS." Revista Mexicana De Ingenieria Quimica **10**(3): 455-463.

Hill, L. E., C. Gomes, et al. (2013). "Characterization of beta-cyclodextrin inclusion complexes containing essential oils (trans-cinnamaldehyde, eugenol, cinnamon bark, and clove bud extracts) for antimicrobial delivery applications." Lwt-Food Science and Technology **51**(1): 86-93.

Hinchliffe, D. J. and J. D. Kemp (2002). "beta-zein protein bodies sequester and protect the 18-kDa delta-zein protein from degradation." Plant Science **163**(4): 741-752.

Ho, C. L. and Y. C. Su (2012). "Composition, Antioxidant and Antimicrobial Activities of the Leaf Essential Oil of Machilus japonica from Taiwan." Natural Product Communications **7**(1): 109-112.

Holley, R. A. and D. Patel (2005). "Improvement in shelf-life and safety of perishable foods by plant essential oils and smoke antimicrobials." Food Microbiology **22**(4): 273-292.

Hong, D. Y., Y. K. Hwang, et al. (2009). "Porous Chromium Terephthalate MIL-101 with Coordinatively Unsaturated Sites: Surface Functionalization, Encapsulation, Sorption and Catalysis." Advanced Functional Materials **19**(10): 1537-1552.

Hu, Y., Y. M. Du, et al. (2009). "Self-aggregation of water-soluble chitosan and solubilization of thymol as an antimicrobial agent." Journal of Biomedical Materials Research Part A **90A**(3): 874-881.

Hulin, V., A. G. Mathot, et al. (1998). "Antimicrobial properties of essential oils and flavour compounds." Sciences Des Aliments **18**(6): 563-582.

Ibrahim, S. A., M. M. Salameh, et al. (2006). "Application of caffeine, 1,3,7-trimethylxanthine, to control Escherichia coli O157 : H7." Food Chemistry **99**(4): 645-650.

Jia, C., X. X. Yuan, et al. (2009). "Metal-Organic Frameworks (MOFs) as Hydrogen Storage Materials." Progress in Chemistry **21**(9): 1954-1962.

Juan-Alcaniz, J., J. Gascon, et al. (2012). "Metal-organic frameworks as scaffolds for the encapsulation of active species: state of the art and future perspectives." Journal of Materials Chemistry **22**(20): 10102-10118.

Juneja, V. K., H. P. Dwivedi, et al. (2012). Novel Natural Food Antimicrobials. Annual Review of Food Science and Technology, Vol 3. M. P. Doyle and T. R. Klaenhammer. **3:** 381-403.

Kalemba, D. and A. Kunicka (2003). "Antibacterial and antifungal properties of essential oils." Current Medicinal Chemistry **10**(10): 813-829.

Kim, C. S., Y. M. Woo, et al. (2002). "Zein protein interactions, rather than the asymmetric distribution of zein mRNAs on endoplasmic reticulum membranes, influence protein body formation in maize endosperm." Plant Cell **14**(3): 655-672.

Kim, S. and D. Y. C. Fung (2004). "Antibacterial effect of crude water-soluble arrowroot (Puerariae radix) tea extracts on food-borne pathogens in liquid medium." Letters in Applied Microbiology **39**(4): 319-325.

Kumar, H., S. K. Tripathi, et al. (2009). "Synthesis, Characterization and Application of Coatings Based on Epoxy Novolac and Liquid Rubber Blend." E-Journal of Chemistry **6**(4): 1253-1259.

Kuo, Y. L., L. Cheng, et al. (2011). "Clinical impact of BI-RADS classification in Taiwanese breast cancer patients: BI-RADS 5 versus BI-RADS 0-4." Eur J Radiol.

Lee, D. U. (2009). "Effects of Combination Treatments of Nisin and High-intensity Ultrasound with High Pressure on the Functional Properties of Liquid Whole Egg." Food Science and Biotechnology **18**(6): 1511-1514.

Li, B. Y., Y. M. Zhang, et al. (2012). "A strategy toward constructing a bifunctionalized MOF catalyst: post-synthetic modification of MOFs on organic ligands and coordinatively unsaturated metal sites." Chemical Communications **48**(49): 6151-6153.

LisBalchin, M. and S. G. Deans (1997). "Bioactivity of selected plant essential oils against Listeria monocytogenes." Journal of Applied Microbiology **82**(6): 759-762.

Luo, Y. C., B. C. Zhang, et al. (2011). "Preparation and characterization of zein/chitosan complex for encapsulation of alpha-tocopherol, and its in vitro controlled release study." Colloids and Surfaces B-Biointerfaces **85**(2): 145-152.

Mastromatteo, M., G. Barbuzzi, et al. (2009). "Controlled release of thymol from zein based film." Innovative Food Science & Emerging Technologies **10**(2): 222-227.

Mathlouthi, N., T. Bouzaienne, et al. (2012). "Use of rosemary, oregano, and a commercial blend of essential oils in broiler chickens: In vitro antimicrobial activities and effects on growth performance." Journal of Animal Science **90**(3): 813-823.

Miguel, M. G., C. Cruz, et al. (2010). "Foeniculum vulgare Essential Oils: Chemical Composition, Antioxidant and Antimicrobial Activities." Natural Product Communications **5**(2): 319-328.

Morita, T., Y. Sakamura, et al. (2000). "Protein encapsulation into biodegradable microspheres by a novel S/O/W emulsion method using poly(ethylene glycol) as a protein micronization adjuvant." Journal of Controlled Release **69**(3): 435-444.

Muller, M., S. Turner, et al. (2011). "Au@MOF-5 and Au/MOx@MOF-5 (M = Zn, Ti; x=1, 2): Preparation and Microstructural Characterisation." European Journal of Inorganic Chemistry(12): 1876-1887.

Muller, M., X. N. Zhang, et al. (2009). "Nanometer-sized titania hosted inside MOF-5." Chemical Communications(1): 119-121.

Oliveira, D. R., G. G. Leitao, et al. (2007). "Chemical and antimicrobial analyses of essential oil of Lippia origanoides HBK." Food Chemistry **101**(1): 236-240.

Paparella, A., L. Taccogna, et al. (2008). "Flow cytometric assessment of the antimicrobial activity of essential oils against Listeria monocytogenes." Food Control **19**(12): 1174-1182.

Parris, N., P. H. Cooke, et al. (2005). "Encapsulation of essential oils in zein nanospherical particles." Journal of Agricultural and Food Chemistry **53**(12): 4788-4792.

Piccirillo, C., S. Demiray, et al. (2013). "Chemical composition and antibacterial properties of stem and leaf extracts from Ginja cherry plant." Industrial Crops and Products **43**: 562-569.

Pirbalouti, A. G., G. H. Rahnama, et al. (2011). "Variation in antibacterial activity and phenolic content of Hypericum scabrum L. populations." Journal of Medicinal Plants Research **5**(17): 4119-4125.

Ploegmakers, J., S. Japip, et al. (2013). "Mixed matrix membranes containing MOFs for ethylene/ethane separation Part A: Membrane preparation and characterization." Journal of Membrane Science **428**: 445-453.

Podaralla, S. and O. Perumal (2010). "Preparation of Zein Nanoparticles by pH Controlled Nanoprecipitation." Journal of Biomedical Nanotechnology **6**(4): 312-317.

Podaralla, S. and O. Perumal (2012). "Influence of Formulation Factors on the Preparation of Zein Nanoparticles." Aaps Pharmscitech **13**(3): 919-927.

Quispe-Condori, S., M. D. A. Saldana, et al. (2011). "Microencapsulation of flax oil with zein using spray and freeze drying." Lwt-Food Science and Technology **44**(9): 1880-1887.

Regier, M. C., J. D. Taylor, et al. (2012). "Fabrication and characterization of DNA-loaded zein nanospheres." Journal of Nanobiotechnology **10**.

Samperio, C., R. Boyer, et al. (2010). "Enhancement of Plant Essential Oils' Aqueous Solubility and Stability Using Alpha and Beta Cyclodextrin." Journal of Agricultural and Food Chemistry **58**(24): 12950-12956.

Santurio, D. F., M. M. da Costa, et al. (2011). "Antimicrobial activity of spice essential oils against Escherichia coli strains isolated from poultry and cattle." Ciencia Rural **41**(6): 1051-1056.

Sarac, N. and A. Ugur (2008). "Antimicrobial activities of the essential oils of Origanum onites L., Origanum vulgare L. subspecies hirtum (Link) Ietswaart, Satureja thymbra L., and Thymus cilicicus Boiss. & Bal. growing wild in Turkey." Journal of Medicinal Food **11**(3): 568-573.

Schlesier, K., M. Harwat, et al. (2002). "Assessment of antioxidant activity by using different in vitro methods." Free Radical Research **36**(2): 177-187.

Schütze, M., H. Boeing, et al. (2011). "Alcohol attributable burden of incidence of cancer in eight European countries based on results from prospective cohort study." BMJ **342**: d1584.

Sha, J. Q., J. W. Sun, et al. (2012). "Syntheses Study of Keggin POM Supporting MOFs System." Crystal Growth & Design **12**(5): 2242-2250.

Shah, B., P. M. Davidson, et al. (2012). "Nanocapsular Dispersion of Thymol for Enhanced Dispersibility and Increased Antimicrobial Effectiveness against Escherichia coli O157:H7 and Listeria monocytogenes in Model Food Systems." <u>Applied and Environmental Microbiology</u> **78**(23): 8448-8453.

Shah, B., S. Ikeda, et al. (2012). "Nanodispersing thymol in whey protein isolate-maltodextrin conjugate capsules produced using the emulsion-evaporation technique." <u>Journal of Food Engineering</u> **113**(1): 79-86.

Sivropoulou, A., E. Papanikolaou, et al. (1996). "Antimicrobial and cytotoxic activities of Origanum essential oils." <u>Journal of Agricultural and Food Chemistry</u> **44**(5): 1202-1205.

Suhr, K. I. and P. V. Nielsen (2003). "Antifungal activity of essential oils evaluated by two different application techniques against rye bread spoilage fungi." <u>Journal of Applied Microbiology</u> **94**(4): 665-674.

Sun, C. Y., C. Qin, et al. (2013). "Metal-organic frameworks as potential drug delivery systems." <u>Expert Opinion on Drug Delivery</u> **10**(1): 89-101.

Suzuki, T., E. Sato, et al. (1989). "Preparation of Zein Microspheres Conjugated with Antitumor Drugs Available for Selective Cancer-Chemotherapy and Development of a Simple Colorimetric Determination of Drugs in Microspheres." <u>Chemical & Pharmaceutical Bulletin</u> **37**(4): 1051-1054.

Tadtong, S., S. Suppawat, et al. (2012). "Antimicrobial Activity of Blended Essential Oil Preparation." <u>Natural Product Communications</u> **7**(10): 1401-1404.

Ultee, A., M. H. J. Bennik, et al. (2002). "The phenolic hydroxyl group of carvacrol is essential for action against the food-borne pathogen Bacillus cereus." <u>Applied and Environmental Microbiology</u> **68**(4): 1561-1568.

van Vuuren, S. F., L. C. du Toit, et al. (2010). "Encapsulation of Essential Oils within a Polymeric Liposomal Formulation for Enhancement of Antimicrobial Efficacy." <u>Natural Product Communications</u> **5**(9): 1401-1408.

Vera, R. R. and J. Chane-Ming (1999). "Chemical composition of the essential oil of marjoram (Origanum majorana L.) from Reunion Island." <u>Food Chemistry</u> **66**(2): 143-145.

Viuda-Martos, M., A. El Gendy, et al. (2010). "Chemical Composition and Antioxidant and Anti-Listeria Activities of Essential Oils Obtained from Some Egyptian Plants." <u>Journal of Agricultural and Food Chemistry</u> **58**(16): 9063-9070.

Wang, C., L. G. Sun, et al. (2012). "Study of the first POM columns pillared MOFs derivative." <u>Inorganic Chemistry Communications</u> **18**: 75-78.

Wang, H. J., Z. X. Lin, et al. (2005). "Heparin-loaded zein microsphere film and hemocompatibility." <u>Journal of Controlled Release</u> **105**(1-2): 120-131.

Ward, S. M., P. J. Delaquis, et al. (1998). "Inhibition of spoilage and pathogenic bacteria on agar and pre-cooked roast beef by volatile horseradish distillates." <u>Food Research International</u> **31**(1): 19-26.

Wu, Y. P., Y. G. Luo, et al. (2012). "Antioxidant and antimicrobial properties of essential oils encapsulated in zein nanoparticles prepared by liquid-liquid dispersion method." <u>Lwt-Food Science and Technology</u> **48**(2): 283-290.

Yanishlieva, N. V., E. M. Marinova, et al. (1999). "Antioxidant activity and mechanism of action of thymol and carvacrol in two lipid systems." <u>Food Chemistry</u> **64**(1): 59-66.

Yin, M. C. and W. S. Cheng (2003). "Antioxidant and antimicrobial effects of four garlic-derived organosulfur compounds in ground beef." <u>Meat Science</u> **63**(1): 23-28.

Yoo, Y., V. Varela-Guerrero, et al. (2011). "Isoreticular Metal-Organic Frameworks and Their Membranes with Enhanced Crack Resistance and Moisture Stability by Surfactant-Assisted Drying." Langmuir **27**(6): 2652-2657.

Young, S. L. (2004). "Natural product herbicides for control of annual vegetation along roadsides." Weed Technology **18**(3): 580-587.

Zenasni, L., H. Bouidida, et al. (2008). "The essentials oils and antimicrobial activity of four nepeta species from Morocco." Journal of Medicinal Plants Research **2**(5): 111-114.

Zhang, B. C., Y. C. Luo, et al. (2010). "Development of Silver-Zein Composites as a Promising Antimicrobial Agent." Biomacromolecules **11**(9): 2366-2375.

Zhao, F. H., Y. X. Che, et al. (2012). "Two metal-organic frameworks (MOFs) based on binuclear and tetranuclear units: Structures, magnetism and photoluminescence." Inorganica Chimica Acta **384**: 170-175.

Zhao, Z. X., Q. B. Xia, et al. (2011). "Role of Temperature in the Structure of Zn(II)-1,4,-BDC Metal-Organic Frameworks and their Adsorption and Diffusion Properties for Carbon Dioxide." Separation Science and Technology **46**(8): 1337-1345.

Zhong, Q. X., H. L. Tian, et al. (2009). "Encapsulation of Fish Oil in Solid Zein Particles by Liquid-Liquid Dispersion." Journal of Food Processing and Preservation **33**(2): 255-270.

Zhou, Y. X., S. G. Liang, et al. (2010). "Synthesis of Asymmetrical Organic Carbonates Catalyzed by Metal Organic Frameworks." Acta Physico-Chimica Sinica **26**(4): 939-945.

Zhu, J. W., X. P. Zeng, et al. (2006). "Adult repellency and larvicidal activity of five plant essential oils against mosquitoes." Journal of the American Mosquito Control Association **22**(3): 515-522.